

# Low-Temperature Photomagnetolectric Properties of Gold-Doped *n*-Type Silicon<sup>†</sup>

J. Agraz-G.\* and S. S. Li

University of Florida, Gainesville, Florida 32601

(Received 11 February 1970)

The photomagnetolectric (PME) effect was observed between 21 and 84 °K in silicon doped with gold and phosphorus. A generalized diffusion equation is formulated and solved with the impurity centers included in the charge-balance equation and arbitrary intensity of steady illumination. When the carrier densities are much smaller than the gold density, the charged impurities maintain charge neutrality, and this results in a range of injection where  $\Delta p = \Gamma_1 \times \Delta n + \Gamma_2 \Delta n^2$ . If the quadratic term dominates, the PME current is proportional to the  $\frac{4}{3}$  power of the photoconductance. This power law is observed in our measurements, from which we deduce values for the product  $\gamma_{1/2}^{1/2} \tau_n$  between 36 nsec and 63  $\mu$ sec.

## I. INTRODUCTION

The purpose of this study was to investigate the effects of heavy gold doping upon the transport of excess carriers in *n*-type silicon by means of the photomagnetolectric (PME) effect. This effect was observed between 21 and 84 °K in gold- and phosphorus-doped silicon, and the small-Hall-angle theory<sup>1</sup> has been extended to account for the effects of the impurities.

For constant recombination lifetime, no trapping and constant ambipolar diffusivity, the PME short-circuit current is proportional to the photoconductivity.<sup>1</sup> The PME effect has been studied in silicon under these conditions for small<sup>2</sup> and large signal.<sup>3, 4</sup> The trapping by the gold centers has significant effects on the diffusion of excess carriers when the equilibrium carrier density is smaller than the gold density. This case occurs in silicon overcompensated by gold at room temperature and in undercompensated silicon at very low temperatures. Our experiments at low temperature show a PME short-circuit current proportional to the  $\frac{4}{3}$  power of the photoconductance. This power law is also obtained from our theoretical analysis.

## II. THEORY

The experimental situation is schematically shown in Fig. 1. The theory for the PME effect<sup>1</sup> involves the solution of the continuity equation for the carriers injected at the illuminated surface. We have obtained this solution under the following assumptions: (i) The magnetic flux density is very small; (ii) the carriers diffuse in one direction only; (iii) photoinjection and surface recombination can be represented as surface boundary conditions; (iv) charge neutrality is preserved and results in a relationship between the excess densities of electrons and holes; (v) the recombi-

tion rate is a function of injection only; and (vi) the injected carriers do not reach the dark surface.

### A. Charge Neutrality

For charge neutrality, the injection-dependent densities must satisfy the equation

$$p + N_{Au}^+ + N_D = n + N_{Au}^- + n_D, \quad (1)$$

where  $N_{Au}^+$ ,  $N_{Au}^-$  denote the density of positively and negatively charged gold centers, respectively.

A detailed solution of this equation is reported elsewhere.<sup>5</sup> Here we only consider the results of

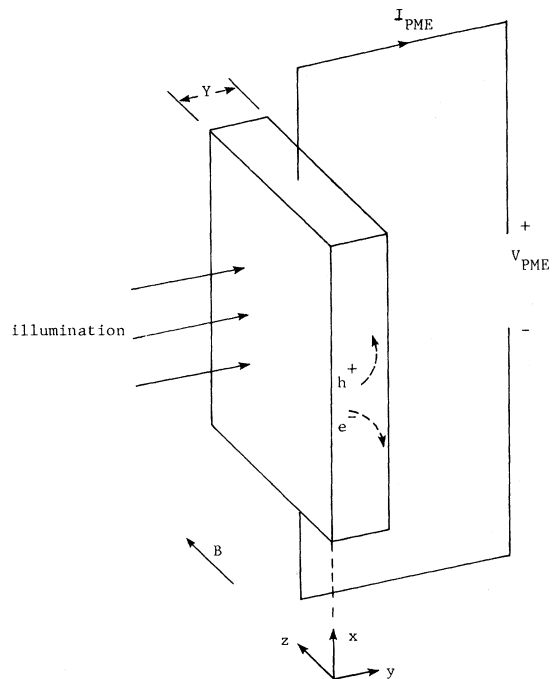


FIG. 1. Schematic sample configuration for the PME and photoconductivity measurements.

direct interest to our experimental work on the PME current and photoconductivity measurements.

Shockley-Read<sup>6</sup> (S-R model) and Sah-Shockley<sup>7</sup> (S-S model) statistics are used to relate the densities of the electrons trapped in the impurity centers to the densities of free carriers. A relationship between the excess carrier densities  $\Delta p$  and  $\Delta n$  can be deduced from Eq. (1) by making use of S-R and S-S statistics, which takes the simple form of power laws within certain ranges of injection.<sup>5</sup> Of particular interest here, are the low-temperature results. The low and moderate injection solution of Eq. (1) takes the form

$$\Delta p = \Gamma_1 \Delta n + \Gamma_2 \Delta n^2, \quad (2)$$

where

$$\Gamma_1 = |N_D - N_{Au}| / (N_D \gamma_{1/2}). \quad (3)$$

$\gamma_{1/2}$  denotes ratio of the hole and electron capture rate for the gold acceptor levels (i. e.,  $\gamma_{1/2} = C_p^- / C_n^+$ ) and

$$\Gamma_2 = \Gamma_1 / n_0 \quad \text{for } N_D > N_{Au}, \quad (4)$$

$$\Gamma_2 = N_{Au} / N_D n_{1D} \gamma_{1/2} \quad \text{for } N_D < N_{Au}. \quad (5)$$

This solution is valid for

$$0 < \Delta n \ll [\Gamma_2 (\gamma_{1/2} \gamma_{-1/2})^{1/2}]^{-1} \quad (6)$$

(where  $\gamma_{-1/2} = C_p^+ / C_n^-$  is the ratio of hole and electron capture rate at gold donor levels) and can be separated into a small injection linear range (i. e.,  $\Delta p \cong \Gamma_1 \Delta n$ ) and an intermediate quadratic range (i. e.,  $\Delta p \cong \Gamma_2 \Delta n^2$ ).

This analysis also shows that the electron recombination lifetime changes slowly with injection.<sup>5</sup>

### B. Diffusion Equation

The PME current is related to the diffusion current, and the photoconductivity is proportional to the average injected carrier density. The continuity equation for electrons is given by

$$\frac{dJ_{ny}}{dy} + qR = 0, \quad (7)$$

where  $R$  denotes the recombination rate,

$$J_{ny} = qn\mu_n E_y + qD_n \frac{dn}{dy} \quad (8)$$

$$\text{and } J_{py} = qp\mu_p E_y - qD_p \frac{dp}{dy}. \quad (9)$$

The Demer field ( $E_y$ ) in Eqs. (8) and (9) is independent of  $y^1$  and the total current in the  $y$  direction is zero. With these considerations, Eqs. (8) and (9) can be reduced to

$$J_{ny} = qD \frac{dn}{dy}, \quad (10)$$

where

$$D = D_n \left( p + n \frac{dp}{dn} \right) / (p + bn)$$

and

$$p = p_0 + \Delta p, \quad n = n_0 + \Delta n \quad (11)$$

is a generalized diffusivity function. The continuity equation in Eq. (7) then takes the form

$$\frac{d}{dy} \left( D \frac{dn}{dy} \right) + R = 0. \quad (12)$$

The solution of Eq. (12) gives an implicit expression for the carrier profile,

$$y = Y - \int_{\Delta n}^{\Delta n_0} D d\Delta n / (2 \int DR d\Delta n + C_1)^{1/2}. \quad (13)$$

The constants of integration are determined by the boundary conditions at the illuminated and dark surfaces. If the injected carriers do not reach the back surface, the constant of integration  $C_1$  is zero. This can be shown from the boundary condition at this surface,

$$q^{-1} j_{nr} + S_d \Delta n_Y = 0, \quad (14)$$

where  $S_d$  is the surface recombination velocity at the dark surface.

Usually the computation of Eq. (13) is only an intermediate step in the calculation of a measurable quantity. Therefore, a complete evaluation of this solution is not necessary.

### C. PME Effect and Photoconductance

The PME short-circuit current per unit sample width, in the limit of small magnetic flux density is<sup>1</sup>

$$I_{PME} = -\theta \int_0^Y J_{ny} dy, \quad (15)$$

where  $\theta = |\theta_n| + |\theta_p|$ ,  $\theta_n = -\mu_{nH} B$ ,  $\theta_p = \mu_{pH} B$ ,

and  $Y$  is the thickness of the sample. For the thick sample, using Eq. (10) we can write

$$I_{PME} = \theta \int_0^{\Delta n_0} qD d\Delta n, \quad (16)$$

where  $\Delta n_0$  is the injected electron density at the illuminated surface.

Similarly the photoconductance can be written as

$$\Delta G = q\mu_n \int_0^Y (\Delta n + \Delta p/b) dy, \quad (17)$$

$$\text{or } \Delta G = q\mu_n \int_0^{\Delta n_0} \left( \Delta n + \frac{\Delta p}{b} \right) \frac{D d\Delta n}{[2 \int_0^{\Delta n} DR d\Delta n]^{1/2}}. \quad (18)$$

Eqs. (16) and (18) relate  $I_{PME}$  and  $\Delta G$  parametrically through  $\Delta n_0$ . In the low-injection linear range  $\Delta p = \Gamma_1 \Delta n$ . Solving Eqs. (10), (11), (16), and (17) one finds

$$I_{\text{PME}} = \frac{\theta(D_1/\tau_n)^{1/2}}{\mu_n(1 + \Gamma_1/b)} \cdot \Delta G = \frac{\theta q D_1 Q_0}{S_i + D_1/\tau_n}, \quad (19)$$

where

$$D_1 = D_n [(n + \Delta n) \Gamma_1 / (bn + \Gamma_1 \Delta n)] . \quad (20)$$

Eq. (19) is consistent with the result obtained by Amith.<sup>8</sup>

Equation (19) predicts a linear relationship between  $I_{\text{PME}}$  and  $\Delta G$ . In this range, the photoconductance, PME current and the photon flux density are proportional to the first power of the surface injection (and therefore to each other). The effective diffusivity ( $D_1$ ) and the lifetime were found to be constant in this range. The linear relationship between  $I_{\text{PME}}$  and  $\Delta G$  has been observed recently by Li<sup>4</sup> in  $n$ -type silicon at low temperatures.

In the intermediate injection range, where the steady-state trapping of photoinjected carriers by gold centers becomes significant, the relation between  $\Delta p$  and  $\Delta n$  is quadratic, i. e.,

$$\Delta p = \Gamma_2 \Delta n^2 . \quad (21)$$

By substituting Eq. (21) into (11) and realizing the fact that in this region  $\Delta p \gg p_0$ ,  $\Delta n \gg n_0$ , and  $\Delta p < \Delta n$ , the diffusivity function  $D$  in Eq. (11) reduces to the form

$$D = (3D_n \Gamma_2 / b) \Delta n . \quad (22)$$

Substituting Eq. (22) into Eq. (16) yields the PME short-circuit current

$$I_{\text{PME}} = \theta (3D_n \Gamma_2 q / b) (\Delta n_0)^2 . \quad (23)$$

And by substituting Eq. (22) and  $R = \Delta n / \tau_n$  into Eq. (18) one finds

$$\Delta G = \mu_n q (2\Gamma_2 D_n \tau_n / b)^{1/2} (\Delta n_0)^{3/2} . \quad (24)$$

From Eqs. (23) and (24), the relationship between  $I_{\text{PME}}$  and  $\Delta G$  is given in the following form:

$$I_{\text{PME}} = \frac{3}{2} \theta q (\Gamma_2 D_n / 4\tau_n^2 b)^{1/3} (\Delta G / q \mu_n)^{4/3} , \quad (25)$$

which predicts a  $\frac{4}{3}$  power law between  $I_{\text{PME}}$  and  $\Delta G$ . This power-law relationship was observed in gold-doped  $n$ -type silicon at low temperatures as will be reported in Sec. III.

### III. EXPERIMENTAL RESULTS AND DISCUSSION

We report here the experimental results on three gold-doped silicon samples. The samples

were prepared by diffusion of gold into phosphorus-doped silicon bars. The impurity concentrations, listed in Table I, were estimated from Hall data obtained between 20 and 300 °K.

By comparing the Hall data of the different samples and the gold diffusion data, we arrive at values for the phosphorus and gold densities as listed in Table I. The activation energy listed is deviated from the accepted value of 0.044 eV for phosphorus at low donor concentrations. However, it is consistent with measurements by Long and Myers<sup>9</sup> of 0.043 eV for a donor concentration of  $4.5 \times 10^{15}$  cm<sup>-3</sup> and by Swartz,<sup>10</sup> who obtained 0.032 eV for  $1.8 \times 10^{17}$  cm<sup>-3</sup> of donor concentration. The activation energy of the phosphorus is estimated for samples 1–3 from the slope of the low-temperature plot of  $R_H T^{3/2}$  versus  $1/T$ , which yields a value of 0.033 eV.

To check the adequacy of our model, we investigate the temperature dependence of the PME short-circuit current  $I_{\text{PME}}$  and compare it with the theoretical expression. From Eq. (25) we find that

$$I_{\text{PME}} \propto \Gamma_2^{1/3} . \quad (26)$$

This is the factor that contributes most to the dependence of  $I_{\text{PME}}$  on temperature because

$$\Gamma_2 = N_{\text{Au}} / N_D \gamma_{1/2} n_{1D} , \quad (27)$$

where

$$n_{1D} = N_C \exp[-(E_C - E_D)/kT] . \quad (28)$$

Since  $n_{1D}$  decreases exponentially with temperature with the activation energy of the phosphorus level, it is found from Eqs. (26) and (27) that  $I_{\text{PME}}$  should increase with decreasing temperature with one-third of the activation energy of phosphorus. The observed  $I_{\text{PME}}$  for  $\Delta G = 0.1$  mho/cm in sample 3 is plotted in Fig. 2. The slope indicated is 0.01 eV which is about one-third of the activation energy we observed for phosphorus. This is in good agreement with the results obtained from the Hall measurements. The experimental procedures for the PME and photoconductance measurements were described in detail previously.<sup>3,4</sup>

In sample 1, gold was diffused at 1200 °C and annealed at 800 °C. This resulted in a light compensation by gold. This sample shows normal band conductivity in the liquid-hydrogen tempera-

TABLE I. Impurity concentrations from Hall-effect, conductivity, and gold-diffusion data.

	$N_D - N_A$ (cm <sup>-3</sup> )	$E_D$ (meV)	$N_A$ (cm <sup>-3</sup> )	$N_D$ (est.) (cm <sup>-3</sup> )	$N_{\text{Au}}$ (est.) (cm <sup>-3</sup> )
Sample 1	$1.7 \times 10^{17}$	33	$10^{16}$	$1.8 \times 10^{17}$	$< 10^{16}$
Sample 2	$8.9 \times 10^{16}$	33	$1.8 \times 10^{17}$	$1.8 \times 10^{17}$	$8 \times 10^{16}$
Sample 3	...	...	...	$2 \times 10^{16}$	$5 \times 10^{16}$

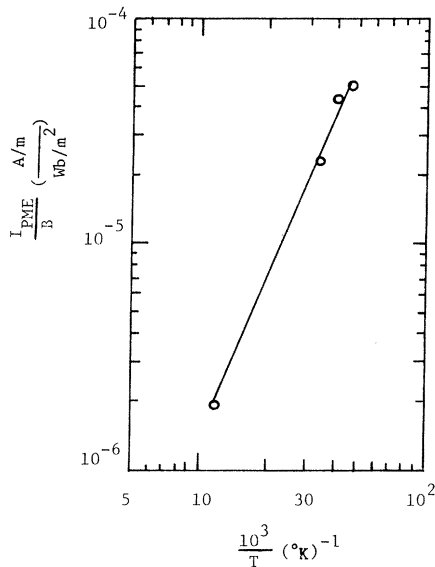


FIG. 2. Temperature dependence of the PME current in sample 3 ( $\Delta G = 0.1 \mu\text{mho}$ ); the slope yields  $E_D = 0.03 \text{ eV}$ .

tures. The mobility increases monotonically with decreasing temperature, consistent with the theory for small compensation. The PME short-circuit current at  $24.7^\circ\text{K}$  is proportional to the  $\frac{4}{3}$  power of the photoconductance, which is consistent with our theory for the range of injection where  $\Delta\phi \propto \Delta n^2$ . This result is shown in Fig. 3.

Sample 2 was prepared by diffusing gold at  $1200^\circ\text{C}$  and then quenching to room temperature. The compensation of phosphorus by gold for this case was about 50%. Impurity conduction by hopping was observed below  $22^\circ\text{K}$ , mixed impurity and band conduction between  $22$  and  $32^\circ\text{K}$  and normal band conduction above  $32^\circ\text{K}$ . The PME current follows the  $\frac{4}{3}$  power law at  $32^\circ\text{K}$ , but shows anomalous behavior below  $29.3^\circ\text{K}$ , where the impurity conduction becomes important. This anomalous behavior is attributed to the interaction of injected carriers with impurity conduction.

In sample 3, gold was diffused at  $1200^\circ\text{C}$  and quenched to room temperature. The gold over-compensation observed in this sample establishes the gold concentration by this diffusion method at about  $5 \times 10^{16} \text{ cm}^{-3}$ . The  $\frac{4}{3}$  power law was observed between  $20.8$  and  $84^\circ\text{K}$ , in good agreement with our model [see Eq. (25)].

A nonlinear PME effect in gold-doped silicon has been observed in the injection range characterized by a  $\frac{4}{3}$  power law for the PME current dependence on the photoconductance. This power-law dependence is related to the steady-state trapping of the photoinjected carriers by the gold centers. From Eq. (25) and the results shown in

TABLE II. The  $(\gamma_{1/2})^{1/2}\tau_n$  product.

	$T$ ( $^\circ\text{K}$ )	$(\gamma_{1/2})^{1/2}\tau_n$ ( $\mu\text{sec}$ )
Sample 1	24.7	63
Sample 2	30.1	0.71
Sample 3	84.0	0.036
	30.4	0.075
	26.0	0.098
	21.6	0.362
	20.8	0.448

Figs. 3–5, one can deduce the electron effective lifetime  $(\gamma_{1/2})^{1/2}\tau_n$ . The corresponding values are listed in Table II.

Since no data are available in literature for the ratio of electron- and hole-capture rate  $\Gamma_{1/2}$  at the gold acceptor centers at low temperatures, it is impossible to calculate the electron lifetime  $\tau_n$  from the PME and PC measurements for the present case. However, it is possible to determine  $\tau_n$  from the photoconductivity decay experiment at low temperature and then to calculate the  $\gamma_{1/2}$  from the PME and PC measurements. The increase in temperature of  $(\gamma_{1/2})^{1/2}\tau_n$  for sample 3 is consistent with the fact that  $\gamma_{1/2}$  increases with temperature because  $C_p^*$  increases faster with temperature than  $C_n^*$ .

The PME open-circuit voltage observed in the gold-doped silicon is found several orders of mag-

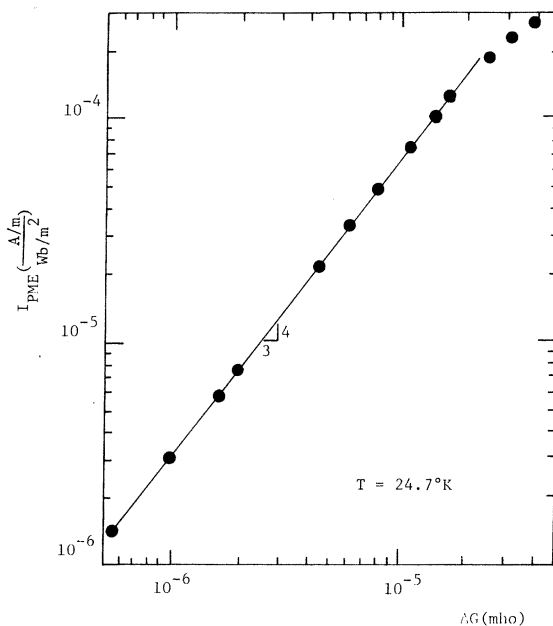


FIG. 3. PME short-circuit current versus photoconductance for sample 1.  $N_D = 1.8 \times 10^{17} \text{ cm}^{-3}$ ,  $N_{\text{Au}} < 10^{16} \text{ cm}^{-3}$ .

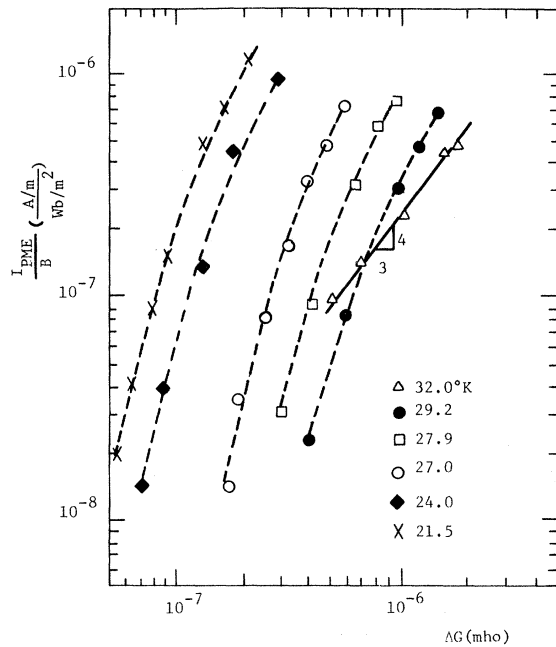


FIG. 4. PME short-circuit current versus photoconductance for sample 2.  $N_D = 1.8 \times 10^{17} \text{ cm}^{-3}$ ,  $N_{Au} \approx 8 \times 10^{16} \text{ cm}^{-3}$ .

nitude greater than that observed in samples without gold.<sup>2-4</sup> The formulation for the steady-state

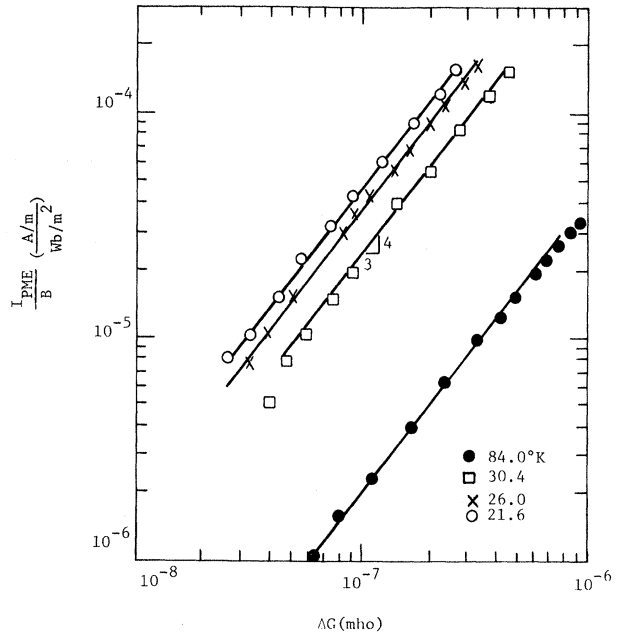


FIG. 5. PME short-circuit current versus photoconductance for sample 3.  $N_D = 2 \times 10^{16} \text{ cm}^{-3}$ ,  $N_{Au} \approx 5 \times 10^{16} \text{ cm}^{-3}$ .

diffusion equation shown here is general with respect to trapping and recombination processes.

†Research supported by the Advanced Research Projects Agency, Department of Defense and monitored by the Air Force Cambridge Research Laboratories under Contract No. F 19628-68-C-0058.

\*Present address: Bell Telephone Laboratories, Inc., Allentown, Pa.

<sup>1</sup>W. van Roosbroeck, Phys. Rev. **101**, 1713 (1956).

<sup>2</sup>M. Ishigame, J. Appl. Phys. (Japan) **3**, 720 (1964).

<sup>3</sup>S. S. Li and C. Wang, *The Proceedings of the Third Photoconductivity Conference*, edited by E. M. Pell

(Pergamon, New York, 1970).

<sup>4</sup>S. S. Li, Phys. Rev. **188**, 1246 (1969).

<sup>5</sup>J. Agraz-G and S. S. Li, Phys. Rev. (to be published).

<sup>6</sup>W. Shockley and W. T. Read, Jr., Phys. Rev. **87**, 835 (1952).

<sup>7</sup>C. T. Sah and W. Shockley, Phys. Rev. **109**, 1103 (1958).

<sup>8</sup>A. Amith, Phys. Rev. **119**, 636 (1960).

<sup>9</sup>D. Long and J. Myers, Phys. Rev. **115**, 1107 (1959).

<sup>10</sup>G. A. Swartz, J. Phys. Chem. Solids **12**, 245 (1960).